

Neutron-mirror neutron oscillations in stars

Wanpeng Tan*

*Department of Physics, Institute for Structure and Nuclear Astrophysics (ISNAP),
and Joint Institute for Nuclear Astrophysics -
Center for the Evolution of Elements (JINA-CEE),
University of Notre Dame, Notre Dame, Indiana 46556, USA*

(Dated: September 16, 2020)

Abstract

Based on a newly proposed mirror-matter model of neutron-mirror neutron ($n - n'$) oscillations [Phys. Lett. B 797, 134921 (2019)], evolution and nucleosynthesis in single stars under a new theory is presented. In the new model, $n - n'$ oscillations are caused by a very small mass difference between particles of the two sectors. The new theory with the new $n - n'$ model can demonstrate the evolution in a much more convincing way than the conventional belief. In particular, many observations in stars show strong support for the new theory and the new $n - n'$ model. For example, progenitor mass limits and structures for white dwarfs and neutron stars, two different types of core collapse supernovae (II-P and II-L), synthesis of heavy elements, pulsating phenomena in stars, etc, can all be easily and naturally explained under the new theory.

* wtan@nd.edu

8 I. INTRODUCTION

9 After the big bang nucleosynthesis (BBN) [1, 2], only light elements are formed with
10 about one quarter of ${}^4\text{He}$, three quarters of ${}^1\text{H}$, and some trace amounts of ${}^2\text{H}$, ${}^3\text{He}$, and
11 ${}^7\text{Li}$ due to the missing links of stable nuclei at mass $A = 5$ and 8. As it turns out, these
12 primordial elements would serve as fuel to form other isotopes in stars when the conditions
13 of high temperature and density can be met. In stars, hydrogen can be further processed
14 into helium via the so-called pp-chain and CNO reactions [3, 4]. To overcome the mass gaps
15 at $A = 5$ and 8, however, the triple-alpha reaction via the Hoyle state (0^+ at 7.654 MeV in
16 ${}^{12}\text{C}$) [5] is needed to start forming ${}^{12}\text{C}$ and subsequently other heavier elements.

17 Such an elegant picture of nucleosynthesis up to carbon has been firmly established
18 while the current understanding of the formation of the heavier elements beyond carbon
19 in stars is not satisfactory and will be challenged in this work. The conventional view of
20 burning between carbon and iron [5] is through alpha capture reactions like ${}^{12}\text{C}(\alpha, \gamma){}^{16}\text{O}$
21 and fusion reactions starting with ${}^{12}\text{C}+{}^{12}\text{C}$. Since iron group nuclei are the most bound ones,
22 isotopes beyond iron have to be generated via the slow and rapid neutron capture processes
23 (s-process and r-process) [6] under different conditions in stars. Although the studies on
24 neutron capture processes on the heavy nuclei have gained much attention especially after
25 the detection of a neutron star merger event by LIGO and VIRGO [7], better understanding
26 of the path and nucleosynthesis of the intermediate nuclei and the seed nuclei for s- and r-
27 processes and these processes themselves is still in need.

28 It is puzzling if we consider that both ${}^{12}\text{C}(\alpha, \gamma){}^{16}\text{O}$ [8] and ${}^{12}\text{C}+{}^{12}\text{C}$ [9] fusion reactions
29 have been measured with much smaller cross sections than desired and the third most
30 abundant isotope in the Universe is ${}^{16}\text{O}$ instead of ${}^{12}\text{C}$. In terrestrial planets including
31 Earth, ${}^{12}\text{C}$ is surprisingly much rarer compared to abundant or even dominant ${}^{16}\text{O}$. Also
32 intriguingly, studies have shown that s-process has two (main and weak) components [10],
33 r-process nuclei are related to “high-” and “low-frequency” events [11], and core-collapse
34 supernovae can be divided into two categories in terms of light curves [12, 13]. Other
35 enigmatic phenomena include progenitor sizes for white dwarfs and neutron stars, carbon-
36 enhanced metal-poor stars (CEMP) in the early Universe [14, 15], and dramatic oscillatory
37 behavior in stars beyond main sequence such as pulsating variables. All these puzzles in stars
38 indicate possible new physics related to neutrons and have motivated recent development of

39 a new mirror-matter model with neutron-mirror neutron ($n - n'$) oscillations [16].

40 Neutron dark decays [17] or some type of $n - n'$ oscillations [16, 18–21] have become
41 a focus of many research efforts recently, at least partly owing to the 1% neutron lifetime
42 discrepancy between two different experimental techniques [22, 23]. However, the dark decay
43 idea was dismissed shortly by other experimental work [24, 25] making $n - n'$ oscillations the
44 only possible option. One is referred to Ref. [16] for more detailed discussions on this aspect.
45 In particular, an interesting study of $n - n'$ oscillations in neutron stars [26] combined with
46 a detailed analysis of pulsar timings and detection of gravitational waves [27] seems to set a
47 very tight constraint on the effect of $n - n'$ oscillations which will be addressed in this work.

48 Most proposals of the $n - n'$ type of oscillations tried to introduce some sort of very weak
49 and explicit interaction between particles in ordinary and mirror (dark) sectors [28–30]. Such
50 an interaction then results in a small mass splitting of $n - n'$ and hence the oscillations.
51 The issue is that it also inevitably makes the oscillations entangled with magnetic fields
52 in an undesirable way due to the nonzero magnetic moment of neutrons. More and more
53 experiments keep pushing its limit to the extreme [20, 31] and effectively disfavor such ideas.

54 A newly proposed model of $n - n'$ oscillations [16], contrarily, looks at least more viable.
55 It is based on the mirror matter theory (first proposed in Ref. [32], further developed
56 later in Refs. [18, 28–30, 33–37]), that is, two sectors of particles have similar yet separate
57 gauge interactions within their own sector but share the same gravitational force. Such a
58 mirror matter theory has appealing theoretical features. The mirror symmetry is particularly
59 intriguing as the Large Hadron Collider has found no evidence of supersymmetry so far and
60 we may not need supersymmetry as conventionally understood, at least not below energies
61 of 10 TeV.

62 The new mirror-matter model that will be applied in this work can consistently explain
63 various observations in the Universe including the neutron lifetime anomaly and dark-to-
64 baryon matter ratio [16], puzzling phenomena related to ultrahigh-energy cosmic rays [38],
65 baryon asymmetry of the Universe [39], unitarity of the CKM matrix [40], dark energy and
66 the nature of neutrinos [41]. Furthermore, various laboratory experiments using current
67 technology have been proposed [40] to test the new model and measure its few parameters
68 more accurately. The model has also been extended into a set of supersymmetric mirror
69 models under dimensional evolution of spacetime to explain the arrow of time and big bang
70 dynamics [42, 43] and to understand the nature of black holes [44].

71 **II. NEW MIRROR-MATTER MODEL AND $n - n'$ OSCILLATIONS**

72 In this new mirror matter model [16], no explicit cross-sector interaction is introduced,
 73 unlike other $n - n'$ type models. The critical assumption of this model is that the mirror
 74 symmetry is spontaneously broken by the uneven Higgs vacuum in the two sectors, i.e.,
 75 $\langle \phi \rangle \neq \langle \phi' \rangle$, although very slightly (on a relative breaking scale of $\sim 10^{-15}$ – 10^{-14}) [16]. When
 76 fermion particles obtain their mass from the Yukawa coupling, it automatically leads to the
 77 mirror mixing for neutral particles, i.e., the basis of mass eigenstates is not the same as that
 78 of mirror eigenstates, similar to the case of ordinary neutrino oscillations due to the family
 79 or generation mixing. Further details of the model can be found in Ref. [16] and further
 80 development in Refs. [41–43].

81 The time evolution of $n - n'$ oscillations in the mirror representation obeys the Schrödinger
 82 equation,

$$i \frac{\partial}{\partial t} \begin{pmatrix} \phi_n \\ \phi_{n'} \end{pmatrix} = H \begin{pmatrix} \phi_n \\ \phi_{n'} \end{pmatrix} \quad (1)$$

83 where natural units ($\hbar = c = 1$) are used for simplicity, the Hamiltonian H for oscillations
 84 in vacuum can be similarly defined as in the case of normal neutrino flavor oscillations [45],

$$H = H_0 = \frac{\Delta_{nn'}}{2} \begin{pmatrix} -\cos 2\theta & \sin 2\theta \\ \sin 2\theta & \cos 2\theta \end{pmatrix} \quad (2)$$

85 and hence the probability of $n - n'$ oscillations in vacuum is [16],

$$P_{nn'}(t) = \sin^2(2\theta) \sin^2\left(\frac{1}{2}\Delta_{nn'}t\right). \quad (3)$$

86 Here θ is the $n - n'$ mixing angle and $\sin^2(2\theta)$ denotes the mixing strength of about 2×10^{-5} ,
 87 t is the propagation time that is assumed to be much shorter than the neutron β -decay
 88 lifetime, and $\Delta_{nn'} = m_{n2} - m_{n1}$ is the small mass difference of the two mass eigenstates of
 89 about 2×10^{-6} eV [16] or a possible range of $10^{-6} - 10^{-5}$ eV [39]. Note that the equation is
 90 valid even for relativistic neutrons and in this case t is the proper time in the particle's rest
 91 frame.

92 If neutrons travel in medium such as dense interior of a star, the Mikheyev-Smirnov-
 93 Wolfenstein (MSW) matter effect [46, 47] may be important, i.e., coherent forward scattering
 94 with other nuclei can affect the oscillations by introducing an effective interaction term in

95 Hamiltonian,

$$H_I = \begin{pmatrix} V_{eff} & 0 \\ 0 & 0 \end{pmatrix}. \quad (4)$$

96 and the effective potential due to coherent forward scattering can be obtained as

$$V_{eff} = \frac{2\pi}{m_n} \sum_i b_i n_i \quad (5)$$

97 where m_n is the neutron mass, n_i is the number density of nuclei of i -th species in the
98 medium, and b_i is the corresponding bound coherent scattering length as tabulated in Ref.
99 [48]. Therefore, the modified Hamiltonian in medium can be written as,

$$H = H_M = \frac{\Delta_{nn'}}{2} \begin{pmatrix} -\cos 2\theta + V_{eff}/\Delta_{nn'} & \sin 2\theta \\ \sin 2\theta & \cos 2\theta - V_{eff}/\Delta_{nn'} \end{pmatrix} \quad (6)$$

100 and the corresponding transition probability is

$$P_M(t) = \sin^2(2\theta_M) \sin^2\left(\frac{1}{2}\Delta_M t\right) \quad (7)$$

101 where $\Delta_M = C\Delta_{nn'}$, $\sin 2\theta_M = \sin 2\theta/C$, and the matter effect factor is defined as,

$$C = \sqrt{(\cos 2\theta - V_{eff}/\Delta_{nn'})^2 + \sin^2(2\theta)}. \quad (8)$$

102 Other incoherent collisions or interactions in the medium can reset the neutron's oscil-
103 lating wave function or collapse it into a mirror eigenstate, in other words, during mean free
104 flight time τ_f the $n - n'$ transition probability is $P_M(\tau_f)$. The number of such collisions will
105 be $1/\tau_f$ in a unit time. Therefore, the transition rate of $n - n'$ for in-medium neutrons is,

$$\lambda_M = \frac{1}{\tau_f} \sin^2(2\theta_M) \langle \sin^2\left(\frac{1}{2}\Delta_M \tau_f\right) \rangle. \quad (9)$$

106 Note that the matter effect factor C cancels in Eqs. (7-9), i.e., the MSW effect is negligible
107 if the matter density is low enough or the propagation time or reset time is short enough (e.g.,
108 when other interactions dominate). Another important feature of the matter effect is that the
109 $n - n'$ oscillations can become resonant as in the case of normal neutrino flavor oscillations
110 [47]. The resonance condition is $\cos 2\theta = V_{eff}/\Delta_{nn'}$, that is, the effective potential V_{eff}
111 is almost equal to the $n - n'$ mass difference since $\cos 2\theta \sim 1$ for $n - n'$ oscillations. The
112 condition obviously depends on the unknown sign of the mass difference as well, which could
113 be determined in laboratory measurements proposed in Ref. [40]. When it resonates, the
114 effective mixing strength is nearly one compared to the vacuum value of 2×10^{-5} .

115 Similar medium effects could also be caused by the existence of magnetic fields. Unlike
 116 some other mirror matter models that are sensitive to weak magnetic fields [19, 20], the new
 117 model used in this work requires a field of $\sim 10^2$ Tesla to be effective. Typical stars do not
 118 produce such strong fields [49] and the effect is therefore negligible in this study. See Ref.
 119 [40] for further discussion of such effects under super-strong magnetic fields and possible
 120 laboratory studies.

121 III. CHALLENGING CONVENTIONAL UNDERSTANDING OF EVOLUTION 122 OF STARS

123 Now we can apply this model to the evolution and nucleosynthesis of stars. In particular,
 124 single stars are discussed for simplicity and assumed to be composed of pure ordinary matter
 125 initially as it is typical during the formation of inhomogeneities in the early universe and
 126 segregation of ordinary and mirror matter on the scale of galaxies or stars [33–36]. We will
 127 discuss two cases. One is low mass stars ($< 8M_\odot$) which will eventually die as a white
 128 dwarf. The other is more massive stars (between $8 - 20M_\odot$) that will undergo supernova
 129 (SN) explosion where r-process could occur for making half of all heavy elements [11] and
 130 leave a neutron star in the end.

131 For both cases the star burns hydrogen first via the so-called pp-chains and CNO cycles
 132 [3, 4]. This is the longest burning process and can take up to billions of years depending
 133 on its initial mass. Then the ashes of the hydrogen burning, ^4He nuclei, start forming ^{12}C
 134 via the triple- α process [50] at $T = 10^8$ K (9 keV in energy). However, that is where the
 135 proposed new nucleosynthesis theory starts to part ways with the conventional wisdom.

136 All the above processes do not produce neutrons. So we first review all the possible
 137 nuclear reactions for neutron production in stars. The reaction has to be of (X, n) -type
 138 where X may be one of existing nuclei like proton, α , or ^{12}C at this moment. It has to be
 139 energy-releasing, i.e., with a positive Q-value. Some reactions with a slightly negative Q-
 140 value (e.g., > -1 MeV) may contribute as well, especially at higher temperatures. Reaction
 141 rates of such reactions are taken from JINA REACLIB database [51] and listed in Table I
 142 where two reactions with positive Q-values immediately stand out,



TABLE I. Reaction rates $N_A\langle\sigma v\rangle$ in unit of $\text{cm}^3/\text{mol}/\text{s}$ as function of stellar temperature and reaction Q-values are listed for neutron source reactions and the data are taken from JINA REACLIB database [51]. The neutron production efficiency factor f_n is defined as the ratio of the neutron mass to the total mass that goes in the reaction.

T [10^8 K]	$^{13}\text{C}(\alpha, n)$	$^{17}\text{O}(\alpha, n)$	$^{18}\text{O}(\alpha, n)$	$^{22}\text{Ne}(\alpha, n)$	$^{12}\text{C}(^{12}\text{C}, n)$	$^{12}\text{C}(^{16}\text{O}, n)$
1	4.2×10^{-14}	9.1×10^{-20}	1.3×10^{-34}	1.3×10^{-29}	7.8×10^{-135}	4.0×10^{-78}
2	3.3×10^{-8}	2.9×10^{-12}	5.8×10^{-17}	1.3×10^{-16}	1.1×10^{-68}	1.6×10^{-51}
5	7.7×10^{-2}	2.7×10^{-4}	2.4×10^{-5}	1.0×10^{-6}	3.6×10^{-28}	3.8×10^{-29}
10	2.5×10^2	2.0	1.3	6.3×10^{-2}	9.4×10^{-14}	1.4×10^{-17}
Q-value [MeV]	2.216	0.587	-0.697	-0.478	-2.598	-0.424
f_n	$\frac{1}{17}$	$\frac{1}{21}$	$\frac{1}{22}$	$\frac{1}{26}$	$< \frac{1}{24} \times 10\%$	$\frac{1}{28} \times 10\%$

143 where the first one is fairly well studied [52] while the second reaction is not, especially at
144 low temperatures [53, 54]. As shown in Table I, the neutron production efficiency factor f_n
145 defined as the ratio of the neutron mass to the total mass involved in the reaction will be
146 used extensively in the following discussion.

147 Conventional understanding for massive stars believes that the density and temperature
148 are high enough at the end of the 3α process so that it can start the $^{12}\text{C} + ^{12}\text{C}$ fusion reaction,
149 subsequently fusing the resulting heavier nuclei like oxygen, silicon, etc, and eventually
150 making the most bound iron material in the core [55]. In this scenario, although refuted
151 by the proposed new theory, both $^{12}\text{C}(^{12}\text{C}, n)$ and $^{12}\text{C}(^{16}\text{O}, n)$ could play a role in neutron
152 production in stars. Unfortunately, only up to 10% of their total cross sections (with more
153 than 90% going to the emission of protons or alphas instead) [56, 57] produce neutrons
154 making the efficiency factor f_n (shown in Table I) too small to contribute. Also listed in
155 Table I, $^{22}\text{Ne}(\alpha, n)$ has been considered as the neutron source reaction for the weak s-process
156 in massive stars [10].

157 Now let us first see how the $n - n'$ oscillation mechanism works in the conventional
158 picture of nucleosynthesis in low mass stars like our sun. According to the conventional
159 understanding, the star may continue to burn some of ^{12}C to ^{16}O by alpha capture reaction
160 but it can not start carbon + carbon fusion due to insufficient density and temperature [55].
161 The star now has an envelope and burning shells of H and He mixed with CNO elements and

162 a C/O core and eventually at a stage called asymptotic giant branch (AGB) where s-process
 163 occurs for making heavy elements [6]. The neutron source reaction $^{13}\text{C}(\alpha, n)$ operates at the
 164 outer layer of the star and ^{13}C can be created from ^{12}C via $^{12}\text{C}(p, \gamma)^{13}\text{N}(\beta^+)^{13}\text{C}$.

165 The s-process environment is typically regarded as follows: density $\rho \sim 10^3 \text{ g/cm}^3$; tem-
 166 perature $T \sim 10^8 \text{ K}$; neutron number density $n_n \sim 10^8 \text{ /cm}^3$ [58]. For simplicity, we assume
 167 the star has a little iron with a solar abundance that will serve as seed at the start of the
 168 s-process.

169 The mean free flight time τ_f of neutrons in the stellar medium is determined by the
 170 scattering cross sections of nuclei. It can be defined by the scattering rate λ_f as follows,

$$\frac{1}{\tau_f} \equiv \lambda_f = \sum_{\text{all nuclei}} \rho N_A \langle \sigma_{nN} v \rangle Y_N \quad (12)$$

171 where N_A is the Avogadro constant, $\langle \sigma_{nN} v \rangle$ is the thermal average of neutron-nucleus scat-
 172 tering cross section times neutron velocity, and Y_N is the mole fraction of the nucleus (i.e., its
 173 mass fraction divided by the mass number of the nucleus) [55]. The typical neutron-nucleus
 174 scattering cross section is about one barn as it is dominated by the neutron scattering
 175 length for low energy neutrons of $\sim 10 \text{ keV}$. And the neutron velocity under the s-process
 176 temperature (10^8 K) is about $1.3 \times 10^6 \text{ m/s}$.

177 In the outer layer of the AGB where $^{13}\text{C}(\alpha, n)$ operates, the sum of $Y_N \sim 0.1$ is typical
 178 assuming that most of it is made of helium and CNO elements. Therefore, we can easily get
 179 $\tau_f \sim 10^{-9} \text{ s}$ from Eq. (12) for neutrons in the s-process environment and the propagation
 180 factor of Eq. (9) is averaged to 1/2 if we omit the matter effect for now.

181 On the other hand, we also need to calculate the neutron loss rate due to the capture
 182 reactions on heavy nuclei which was the main motivation in the study of the s-process.
 183 Similar to Eq. (12), we can write the neutron loss rate from capture reactions as follows,

$$\lambda_{cap} = \rho N_A \langle \sigma_{cap} v \rangle Y_N \quad (13)$$

184 where the neutron capture reaction rate $N_A \langle \sigma_{cap} v \rangle$ is about $10^3 \text{ cm}^3/\text{mol/s}$ for ^{12}C and about
 185 $10^6 \text{ cm}^3/\text{mol/s}$ for ^{56}Fe at s-process temperature [51]. For capture reaction on ^{56}Fe which
 186 represents the seed for s-process with $Y_{^{56}\text{Fe}} \sim 10^{-5}$ inferred from the solar abundance, the
 187 rate $\lambda_{cap}(^{56}\text{Fe})$ is about 10^4 s^{-1} . The rate is similar for capture reactions on light C/O
 188 nuclei. However, this capture process does not contribute to the loss rate of neutrons since

189 the resulting ^{13}C will release the neutron via (α, n) reaction later. Therefore, the neutron
 190 loss rate due to capture reactions or s-process is $\lambda_{cap} \sim 10^4 \text{ s}^{-1}$.

191 From Eqs. (9) and (13), we can obtain the branching ratio of the neutrons that oscillate
 192 into mirror neutrons to those that are captured into nuclei on the condition that the matter
 193 or medium effect in Eqs. (4-8) is omitted,

$$Br\left(\frac{nn'}{cap}\right) = \frac{\lambda_f}{2\lambda_{cap}} \sin^2(2\theta) \sim 1 \quad (14)$$

194 which indicates that similar amounts of neutrons lost to either $n - n'$ oscillations or s-
 195 process in the beginning. Note that this branching ratio does not depend on the density
 196 because the individual rates depend on the density in the same way and get canceled for
 197 the ratio. Also note that the condition is for the very beginning of s-process. The s-process
 198 is a very slow process as it has to wait for many long-lived nuclei to decay along the path
 199 before it can capture neutrons again [55]. So on average, s-process may only use a small
 200 fraction of all available neutrons and most of the neutrons may go via the $n - n'$ oscillation
 201 process. Additionally, current model simulations [59] typically use very small amounts of
 202 ^{13}C ($10^{-6} - 10^{-5} M_{\odot}$) to reproduce the s-process. This shows evidence that $n - n'$ oscillations
 203 may take away most of produced neutrons.

204 Now we can re-visit the oscillation rate considering the matter effect for the following
 205 conditions: density of 10^3 g/cm^3 with compositions of 10% hydrogen and 90% carbon in
 206 mass, scattering lengths of $b(^1\text{H}) = -3.74 \text{ fm}$ and $b(^{12}\text{C}) = 6.65 \text{ fm}$ [48]. Then the effective
 207 potential can be calculated as $V_{eff} \sim 2 \times 10^{-5} \text{ eV}$. If we assume that the 90% part is made
 208 of both carbon and oxygen evenly, we can obtain $V_{eff} \sim 6 \times 10^{-6} \text{ eV}$ that is amazingly close
 209 to the estimate of the $n - n'$ mass difference of $6.578 \times 10^{-6} \text{ eV}$ assuming equivalence of the
 210 CP violation and mirror symmetry breaking scales [60]. In fact, in slightly outer regions
 211 with lower density of about 10^2 g/cm^3 , or for a possible larger $n - n'$ mass splitting up to
 212 10^{-5} eV [39], V_{eff} and $\Delta_{nn'}$ could be almost identical, i.e., leading to maximal or resonant
 213 oscillations. If resonant n-n' oscillations indeed occur, then we can learn that the sign of
 214 $\Delta_{nn'}$ is positive.

215 Then where do the mirror neutrons go? Taking the similar step as suggested in Ref. [26],
 216 the mirror neutrons converted from the oscillations will travel to the core of the star due to
 217 gravity. The $n - n'$ oscillations are forbidden in bound nuclei due to energy conservation,
 218 but they do occur in stars when neutrons are produced free. However, the neutrons emitted

219 from $^{13}\text{C}(\alpha, n)$ can have energy up to 2.2 MeV and potentially escape from the star if it
 220 oscillates immediately into a mirror neutron. Fortunately, the very short mean free flight
 221 time discussed above makes the neutron thermalized first before oscillating into a mirror
 222 neutron. Its thermal energy is about 8.6 keV at $T = 10^8$ K. During the thermalization
 223 process, the light neutrons (compared to heavy nuclei) could diffuse into outer regions and
 224 probably meet the resonant condition and then maximally oscillate into mirror neutrons as
 225 discussed above. Assuming that the inner part of the star is white-dwarf-like (e.g., $1M_{\odot}$ and
 226 Earth-size), it can provide a gravitational binding energy of ~ 0.2 MeV in addition to the
 227 energy the outer layer can supply should the mirror neutron escape. Therefore, most of the
 228 mirror neutrons will go to the core.

229 Note that mirror neutrons interact with ordinary matter only via gravity, so they become
 230 uniformly mixed with ordinary matter in the core with equal density. The details on the
 231 core evolution will be discussed with the new theory later.

232 One observation on the factor f_n in Table I seems to be particularly interesting. $^{13}\text{C}(\alpha, n)$
 233 converts about 1/17 of the total mass into neutrons. Suppose that all the neutrons oscillate
 234 to mirror neutrons ending up in the core, it means that almost 6% of the star mass will go
 235 into the core in this way. Note that other similar reactions contribute as well. This may
 236 provide a link to connect the Chandrasekhar limit [61] to the mass limit on the progenitor
 237 [12] and will be explored further in the next section.

238 If this indeed is the scenario, our understanding of stellar nucleosynthesis has to be
 239 changed. The CNO elements may have additional functions other than serving as catalyst for
 240 making helium. In particular, the CNO elements ^{13}C and ^{17}O can trigger $n - n'$ oscillations
 241 via (α, n) reaction (with positive reaction Q-values). To a certain extent, $^{18}\text{O}(\alpha, n)$ and
 242 $^{18}\text{O}(\alpha, \gamma)^{22}\text{Ne}(\alpha, n)$ (with a little negative reaction Q-values) at higher temperatures and
 243 other heavier (α, n) reactions like $^{21}\text{Ne}(\alpha, n)$ (with positive reaction Q-values) at later stages
 244 may contribute as well.

245 IV. NEW PICTURE OF STELLAR EVOLUTION WITH $n - n'$ OSCILLATIONS

246 As shown below in the proposed new theory, the neutron production process plays a
 247 critical role in the evolution and nucleosynthesis of a star. The $n - n'$ oscillations dictate how
 248 the degenerate core is formed, how the mass of the progenitor is related to the Chandrasekhar

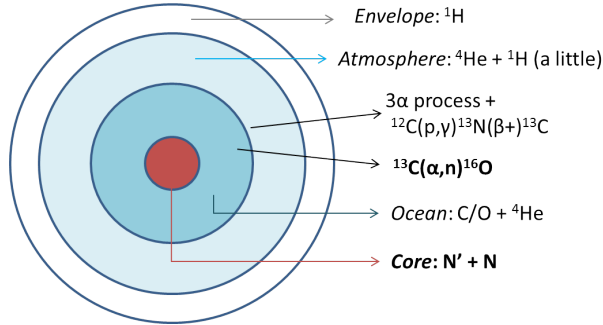


FIG. 1. The schematic diagram is shown for the structure of a red giant star at the first neutron-production $^{13}\text{C}(\alpha, n)$ phase. N and N' in the core stand for evenly mixed matter and mirror matter, respectively.

249 limit and the neutron star mass limit, and possibly why or when the star may explode - a
 250 difficult task for current simulations to do.

251 In the first burning step after the 3α process, starting with $^{13}\text{C}(\alpha, n)$, ^{16}O will be accu-
 252 mulated as ashes from the burning of all carbon nuclei. Then in the second step, hydrogen
 253 fuel is added and $^{16}\text{O}(p, \gamma)^{17}\text{F}(\beta^+)^{17}\text{O}$ will convert ^{16}O into ^{17}O . The second neutron source
 254 reaction $^{17}\text{O}(\alpha, n)$ starts to take effect and converts all oxygen nuclei to neon nuclei. From
 255 both reactions, it effectively converts star matter into mirror neutrons by $(1/17 + 1/21) =$
 256 10% according to the f_n factors shown in Table I. At the same time, both neutron source
 257 reactions could provide a small fraction of neutrons for the s-process. To meet the Chan-
 258 drasekhar limit of about $1.4M_\odot$ for a white dwarf, mirror neutrons cannot exceed $0.7M_\odot$ in
 259 mass or no more than $7M_\odot$ star matter can be burned. There is another $0.7M_\odot$ of ordinary
 260 matter in the core that does not participate in the burning. This sets the higher mass limit
 261 of $7.7M_\odot$ for the progenitor of a white dwarf, or the lower mass limit for the progenitor
 262 of a core-collapse supernova, which is in excellent agreement with the observation limit of
 263 $8 \pm 1M_\odot$ [12].

264 As a matter of fact, the above picture is not unlikely and it is more natural. Taken into
 265 account the rates from Table I at $T = 10^8$ K when the triple- α process starts, one can
 266 see how this could occur. At this moment the star as a red giant has a helium core and
 267 hydrogen envelope and a small amount of hydrogen is mixed in the helium core. The first
 268 step considered here is dictated by the slowest triple- α reaction. Since this burning process
 269 is ignited at the center of the core and gradually moved outwards, the red giant becomes

270 brighter as it evolves. The typical structure of the star at this phase is shown in Fig. 1.

271 When three helium nuclei fuse into a ^{12}C nucleus, it quickly captures a mixed-in proton
272 to become unstable ^{13}N which has a 10-minute β^+ -decay half-life [62]. A possible alternative
273 path via $^{12}\text{C}(\alpha, \gamma)$ (as commonly believed) does not play a role as its reaction rate is 15 orders
274 of magnitude [51] lower than that of $^{12}\text{C}(p, \gamma)$ due to a higher Coulomb barrier. Neither does
275 $^{13}\text{C}(\alpha, \gamma)$. The only requirement is the existence of a small amount of hydrogen. Several
276 scenarios indeed make it plausible. First, for a low metallicity star, i.e., no significant amount
277 of CNO elements present in its initial composition, only pp-chain burns the initial hydrogen.
278 At this point of the star's life, it is probably no more than or close to two times the p-p
279 reaction lifetime. Therefore, we could have more than 10% hydrogen left in the core. Even if
280 significant CNO elements exist and exhaust hydrogen in the core, their highly temperature
281 sensitive reaction rates result in plenty of hydrogen left at lower temperature regions outside
282 the core. The core is not degenerate for stars with $M > 2M_{\odot}$ [63], and the burning can
283 cause convection which could bring in fresh hydrogen from the exterior. If none of the above
284 works, when the triple- α burning front grows out of the small original core $^{12}\text{C}(p, \gamma)$ and
285 subsequently $^{13}\text{C}(\alpha, n)$ can then proceed.

286 The two reasons why ^{13}N waits for its decay instead of capturing another proton: most of
287 the nearby hydrogen has been used up first by ^{12}C ; the $^{12}\text{C}(p, \gamma)$ rate ($\sim 10^{-5}$ cm³/mol/s) is
288 much higher than that of $^{13}\text{N}(p, \gamma)$ ($\sim 10^{-6}$ cm³/mol/s) [51]. In the end, ^{13}N will decay into
289 ^{13}C . If hydrogen is overabundant in the burning region, the CNO cycles will quickly fuse
290 the excess into ^4He that are then burned into ^{12}C and eventually ^{13}C . Because the $^{13}\text{C}(\alpha, n)$
291 rate is ten orders of magnitude higher than the triple- α rate [51], ^{13}C is quickly converted
292 into ^{16}O after the ^{13}N decay on a 10-minute time scale behind the triple- α burning front.
293 Note that the $n - n'$ oscillations effectively make $^{13}\text{C}(\alpha, n)$ a cooling reaction by losing the
294 kinetic energy of the mirror neutron, which may help stabilize the burning front.

295 As discussed earlier, the generated neutrons then oscillate into mirror neutrons that will
296 go in the core mixing evenly with ^{16}O . In addition, some of the mirror neutrons actually
297 oscillate back to ordinary neutrons according to Eqs. (7-9). To calculate the oscillation
298 probability, we assume that, at a later stage, the core as progenitor of a white dwarf has a
299 similar density (10^6 g/cm³), where mirror neutrons can be regarded as a gas of free moving
300 particles governed solely by gravity. Applying the virial theorem on the n' system, one can
301 estimate the mean velocity of mirror neutrons $v' = 2.5 \times 10^{-3}(M'/[\text{g}])^{1/3}$ cm/s which grows

302 as the mirror matter mass M' increases. At some stage, e.g., $M' = 0.1M_\odot$, one can obtain
 303 $v' = 1.5 \times 10^8$ cm/s and hence $\tau'_f \sim 10^{-14}$ s and $\lambda_{n'n} \sim 0.1$ s $^{-1}$. At earlier stages, this reverse
 304 oscillation rate can be several orders of magnitude faster. What it does is it provides free
 305 neutrons to make the ordinary core material more neutron-rich.

306 Initially ^{16}O in the core can be enriched up to its dripline nucleus ^{24}O [64] via $n' \rightarrow n$.
 307 Note that these highly neutron-rich nuclei can not undergo the usual beta decays owing to
 308 electron degeneracy in the core. As found out recently, light neutron-rich nuclei have much
 309 higher fusion cross sections than normal ones [65]. So these enriched oxygen nuclei likely
 310 fuse further into other neutron-rich intermediate nuclei between oxygen and iron or may
 311 further capture the leftover helium near the bottom of the ocean as shown in Fig. 1, at
 312 the same time releasing large amounts of energy. Eventually the core may develop into an
 313 onion-like structure starting from the outside layer of O, then Ne, Si, S, Cr, up to Fe in
 314 the center. When the temperature in the core is high enough as the mass is close to the
 315 Chandrasekhar limit at late burning stages, the core, at least the inner part, may reach a
 316 state of nuclear statistical equilibrium (NSE) consisting of mostly iron-group elements with
 317 a crust of lighter neutron-rich nuclei.

318 Alternatively, mirror neutrons can undergo mirror β -decay $n' \rightarrow p' + e'^- + \bar{\nu}'$ with the same
 319 lifetime of about 888 sec [16]. When the ordinary core matter is fully enriched, i.e., no more
 320 neutrons can be taken, mirror neutrons have to decay to mirror protons. A mirror proton
 321 will fuse immediately with a mirror neutron to make a mirror deuteron. Subsequently, the
 322 mirror core matter will conduct mirror nucleosynthesis similar to the ordinary one, e.g.,
 323 three mirror alphas fuse into one mirror ^{12}C . At the same time, the fusion process on the
 324 ordinary side will produce free neutrons that can oscillate into mirror neutrons to enrich the
 325 mirror matter. Through this mutual oscillation process, both ordinary and mirror matter
 326 will develop into similar evenly-mixed core structures (possibly an iron core at NSE with a
 327 neutron-rich crust in the end) as shown in Fig. 1.

328 The degenerate core's pressure is maintained by both the electron degeneracy and the
 329 large energy release of about 8 MeV per neutron due to nuclear binding energy as the free
 330 neutron from the $^{13}\text{C}(\alpha, n)$ reaction is effectively and ultimately converted into the nuclidic
 331 matter in the core. The Chandrasekhar limit for mixed degenerate ordinary and mirror
 332 matter is smaller than the usual value by a factor of $\sqrt{2}$, which is consistent with the
 333 observed lower mass limit of $\sim 1M_\odot$ for neutron stars [66]. But large amounts of energy

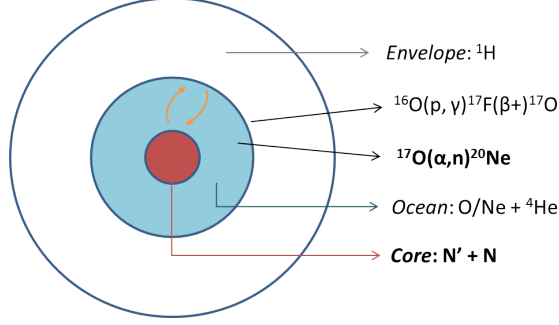


FIG. 2. The schematic diagram is shown for the structure of an AGB star at the second neutron-production $^{17}\text{O}(\alpha, n)$ phase. N and N' in the core stand for evenly-mixed matter and mirror matter, respectively.

334 release (much larger than $\lesssim 0.5$ MeV per nucleon of what conventionally believed fusion
 335 reactions can provide near the core) could make the limit significantly higher and cause
 336 the spread of the neutron star mass distribution. Therefore the average limit could still be
 337 similar, i.e., close to the observed average neutron star mass of $1.4M_{\odot}$.

338 Once all the helium are exhausted or its density is lowered enough to not sustain the
 339 triple- α process, therefore no more $^{13}\text{C}(\alpha, n)$ running, the core stops growing. Without
 340 the heat from the burning and the neutron-conversion process in the core, the core begins
 341 contraction and cools down, pushing away the red giant's hydrogen envelope.

342 When the core settles and starts pulling back the hydrogen envelope, it may go into the
 343 observed AGB phase, i.e., the second burning step that will be discussed below.

344 At the second phase, the outer envelope of hydrogen starts falling in and becoming
 345 compressed on the surface, it can react with the ^{16}O on the surface that was newly formed
 346 in the previous step and still mixed with some helium. The $^{16}\text{O}(p, \gamma)^{17}\text{F}$ reaction makes
 347 ^{17}F nuclei very quickly, which will sink down in the ocean and decay into ^{17}O with a 64.5-
 348 second β^+ -decay half-life [62]. Then the second neutron source reaction of $^{17}\text{O}(\alpha, n)$ starts,
 349 although at a slower rate than the $^{13}\text{C}(\alpha, n)$ rate in the first step. The rate of the only
 350 possible competing reaction $^{17}\text{O}(\alpha, \gamma)$ is 16 orders of magnitude lower at $T = 10^8$ K as
 351 shown by the work of Best *et al.* [53]. The typical structure of the star at the second or
 352 AGB phase is shown in Fig. 2.

353 Note that the difference here is that the second phase burning starts from just outside
 354 and without the helium atmosphere. This probably explains why the AGB stars appear

355 very bright. There may be convection in the ocean to move heavy ash nuclei ^{20}Ne down
 356 and bring ^{16}O back up. However, it is not required since the heavy ^{20}Ne sinks into the core,
 357 exposing the ^{16}O to the envelope again as if the envelope “eating” away the ocean layer
 358 by layer. Eventually the ocean material outside the core will be all processed in this way.
 359 Once no more neutrons are produced, the heat from the neutron-conversion process of $n' - n$
 360 oscillations in the core stops. The star begins contraction again and becomes a white dwarf
 361 composed of evenly mixed ordinary-mirror matter in the end.

362 If the produced mirror neutron matter exceeds $0.7M_{\odot}$ during the above two steps, in
 363 other words, the core weighs beyond the Chandrasekhar limit of about $1.4M_{\odot}$, the red giant
 364 will undergo supernova explosion. As discussed above, the star will need at least $7.7M_{\odot}$
 365 as a progenitor to explode. Before the explosion, the $^{13}\text{C}(\alpha, n)$ and $^{17}\text{O}(\alpha, n)$ reactions in
 366 the two phases naturally provide the neutron sources for the main (slower but longer) and
 367 weak (faster but shorter) s-processes, respectively. After the explosion, the neutron-rich
 368 crust material could be ejected and provide high neutron flux for r-process, which could
 369 explain the abundances of r-process nuclei in early generation of stars and diverse sources
 370 for r-process [11] as discussed below.

371 As for the fate of more massive stars with $M > 8M_{\odot}$, there may actually be double core
 372 collapses for ordinary and mirror matter, respectively. The ordinary and mirror matter will
 373 become a mixture of mirror and ordinary neutrons forming the $n - n'$ star. As shown above,
 374 the core of the star can exceed the Chandrasekhar limit during any of the two phases. So
 375 we should see two types of core-collapse supernovae that can actually be identified with the
 376 observed ones. The cores formed in both cases are essentially the same while the outer layers
 377 are much different and can help distinguish the two types.

378 First, Type II-Plateau supernovae (SNe II-P) have been reported with the following
 379 properties [12, 13]: most common (60%); less peak brightness but with a plateau in light
 380 curve; progenitor of $8 - 15M_{\odot}$; strong hydrogen lines with no helium. This matches exactly
 381 the type of supernovae collapsed in the second phase. Considering $f_n = 1/17$ for the first step
 382 reaction $^{13}\text{C}(\alpha, n)$ as shown in Table I, the star needs to burn at most $12M_{\odot}$ to go through the
 383 first step without reaching the Chandrasekhar limit. Adding $1M_{\odot}$ in the unburned ordinary
 384 core and $2M_{\odot}$ for the outer layers, one gets the upper mass limit of $15M_{\odot}$. Combined with
 385 the lower mass limit from the white dwarf analysis above, this type indeed matches the same
 386 mass range for the less massive supernovae. During the second step, the burning starts from

387 outside making the ocean layer very thick. When the core collapses, it has to blow off the
 388 thick O/Ne ocean layer which will lower its peak luminosity. On the other hand, during
 389 the explosion, the thick O/Ne layer may continue to generate energy by nucleosynthesis and
 390 therefore present itself as the plateau in light curve. The helium atmosphere is gone after the
 391 first step, and the hydrogen envelope is participating directly in burning during the second
 392 step, explaining why hydrogen spectrum lines are strong but no evidence of helium. This
 393 type of SNe may be the “high-frequency” events for heavy r-process nuclei [11].

394 Second, Type II-Linear supernovae’s (SNe II-L) features are as follows [13]: relatively
 395 rare (a few percent); more peak brightness but linear decline in light curve; progenitor
 396 more massive ($> 15M_{\odot}$); evidence of helium; hydrogen lines appearing later and weaker.
 397 This matches exactly the type exploded in the first phase. The very slow triple- α reaction
 398 starts the burning from the core. The subsequent neutron production reaction is much
 399 faster, growing the core accordingly. Therefore, the ocean layer is very thin. When the
 400 star explodes, it just needs to blast away the light helium atmosphere. The result is more
 401 luminosity in the peak and also a quick decline in light curve. Explosions in the first phase
 402 need more mass as discussed above. During the triple- α burning, the hydrogen envelope
 403 was pushed away and hence producing weaker hydrogen lines at a later time. This type
 404 of SNe may be the “low-frequency” events for light r-process nuclei [11]. This type of more
 405 massive SNe may also dominate in the early universe as they evolve faster and large amounts
 406 of neutrons ejected during the explosion can quickly burn the helium layer into carbon via
 407 ${}^4\text{He}+{}^4\text{He}+n \rightarrow {}^9\text{Be}$ and ${}^9\text{Be}(\alpha, n){}^{12}\text{C}$ reactions that are much faster than the triple- α process
 408 [67]. This may enhance the carbon abundance in the early generation of stars leading to the
 409 so-called carbon-enhanced metal-poor (CEMP) stars [15].

410 Neutron star progenitors with mass beyond $20M_{\odot}$ are rarely observed [12]. Under this
 411 theory, we may be able to obtain an upper mass limit for neutron stars from this observation.
 412 The first phase of neutron production in red giants converts about 1/17 of its mass to mirror
 413 neutrons at maximum. For a $20M_{\odot}$ star, therefore, it could end up with a core of $2.22M_{\odot}$. If
 414 $2.22M_{\odot}$ is indeed the limit, then stars need at least $20M_{\odot}$ to collapse into black holes in the
 415 first phase. On the other hand, a star with $15\text{--}20M_{\odot}$ can build a core up to $3\text{--}4M_{\odot}$ during
 416 the second phase and then quietly turns into a black hole in the end. This may explains why
 417 the above-mentioned SNe II-L are so rare. Further studies on the mass limit of neutron stars
 418 and the nature of black holes can be found in Ref. [44] based on supersymmetric mirror

419 extensions of the new model [42, 43].

420 V. FURTHER IMPLICATIONS OF THE NEW THEORY

421 Now the interesting test mentioned in the introductory section [26, 27] can be easily
422 answered. By the time the neutron star (more properly $n - n'$ star) forms, it is already
423 evenly mixed between mirror and ordinary matter. So there is no mass loss or orbital period
424 changing as suggested by Ref. [26]. Therefore, the new theory is consistent with the test of
425 pulsar timings and gravitational wave observations [27]. The surprisingly low carbon content
426 in rocky planets mentioned in Introduction could also be understood if these planets were
427 formed from the ejected debris of type II-P supernovae.

428 Another interesting result that can be obtained under this theory is that oscillating
429 movement from the mirror matter in the star is unavoidable as gravity serves as the restoring
430 force for the oscillations. The oscillating period of the mirror matter can then be written as

$$\text{Period} = \sqrt{\frac{3\pi}{G\rho}} \quad (15)$$

431 where G is the gravitational constant and ρ is the matter density where the mirror particles
432 are located. Due to the gravitational coupling, the ordinary matter has to do the counter
433 movement and therefore presents some kind of pulsating behavior, in particular, periodic
434 changes in luminosity. As a matter of fact, such behaviors are very common in stars,
435 especially in red giants like the Cepheid variables that can be used to determine distances and
436 the compact remnants like neutron stars [68] and even white dwarfs [69]. Such phenomena
437 may help reveal the distribution and movement of mirror matter inside an astrophysical
438 object or understand the laws for the mirror matter. For example, neutron stars have
439 density of about 10^{14} g/cm³ and an oscillation period of $\sim 10^{-3}$ s that can be estimated
440 from Eq. (15) has indeed been observed in neutron stars [68]. The 5-min oscillations from
441 the Sun [70, 71] could also be explained by a small amount of oscillating mirror matter in
442 the center at a density of $\sim 10^3$ g/cm³. The typical period of a red giant variable is between
443 hours and days that can be understood with oscillating mirror matter in its photosphere
444 with a density of $1 - 10^{-3}$ g/cm³ since, as discussed above, the variable star is constantly
445 producing mirror neutrons that can migrate to the photosphere.

446 Such a pulsating behavior in the core that is evenly mixed with ordinary and mirror

447 matter and new understanding of the core structures could shed light on the mechanism of
448 supernova explosions [72, 73]. The large energy release of the neutron-conversion process
449 from $n - n'$ oscillations near the core may also play a role. Meanwhile, the neutron-rich crust
450 may provide an ample neutron source for the revived shock during a supernova explosion
451 for synthesis of heavy elements via r-process. Taking into account new physics of this new
452 star evolution theory, state-of-the-art supernova simulation models could potentially reveal
453 how a core-collapse supernova is exploded.

454 VI. CONCLUSIONS

455 To conclude, the new theory for single star evolution coupled with the $n - n'$ oscillation
456 model is strongly supported by astrophysical observations. $^{13}\text{C}(\alpha, n)^{16}\text{O}$ and $^{17}\text{O}(\alpha, n)^{20}\text{Ne}$
457 are identified as the two critical nuclear reactions for the two-phase late stellar evolution as
458 well as the free neutron sources for main and weak components of s-process, respectively.
459 The mechanism of $n - n'$ oscillations plays an essential role in the formation of the stellar
460 core with mirror matter. Stellar nucleosynthesis, in particular, both s-process and r-process
461 can be understood under the new theory. Progenitor sizes of compact stars and mass limits
462 of neutron stars are also explained. Observed features of the two types of core-collapse
463 supernovae match the predictions of the new mirror matter model well. The mirror matter
464 just like ordinary matter may indeed exist in our universe, especially in stars. This theory
465 could also be applied to the studies for binary or multiple star systems. In particular, Type
466 Ia supernovae, galaxy collisions [74, 75], and recently observed neutron star mergers [7] could
467 be ideal for further test of this theory.

468 ACKNOWLEDGMENTS

469 I would like to thank Ani Aprahamian and Michael Wiescher for supporting me in a
470 great research environment at Notre Dame. I also thank Grant Mathews for pointing out
471 the possibility of mirror neutrons escaping from the star. This work is supported in part
472 by the National Science Foundation under grant No. PHY-1713857 and the Joint Institute
473 for Nuclear Astrophysics (JINA-CEE, www.jinaweb.org), NSF-PFC under grant No. PHY-

-
- 475 [1] R. A. Alpher, H. Bethe, and G. Gamow, *Phys. Rev.* **73**, 803 (1948).
- 476 [2] C. Pitrou, A. Coc, J.-P. Uzan, and E. Vangioni, *Phys. Rep.* **754**, 1 (2018).
- 477 [3] H. A. Bethe and C. L. Critchfield, *Phys. Rev.* **54**, 248 (1938).
- 478 [4] H. A. Bethe, *Phys. Rev.* **55**, 103 (1939).
- 479 [5] F. Hoyle, *Astrophys. J. Suppl. Ser.* **1**, 121 (1954).
- 480 [6] E. M. Burbidge, G. R. Burbidge, W. A. Fowler, and F. Hoyle, *Rev. Mod. Phys.* **29**, 547 (1957).
- 481 [7] LIGO Scientific Collaboration and Virgo Collaboration, B. P. Abbott, R. Abbott, T. D. Ab-
482 bott, F. Acernese, K. Ackley, C. Adams, T. Adams, P. Addesso, R. X. Adhikari, and others,
483 *Phys. Rev. Lett.* **119**, 161101 (2017).
- 484 [8] R. J. deBoer, J. Görres, M. Wiescher, R. E. Azuma, A. Best, C. R. Brune, C. E. Fields,
485 S. Jones, M. Pignatari, D. Sayre, K. Smith, F. X. Timmes, and E. Uberseder, *Rev. Mod.*
486 *Phys.* **89**, 035007 (2017).
- 487 [9] W. P. Tan, A. Boeltzig, C. Dulal, R. J. deBoer, B. Frentz, S. Henderson, K. B. Howard,
488 R. Kelmar, J. J. Kolata, J. Long, and others, *Phys. Rev. Lett.* **124**, 192702 (2020).
- 489 [10] F. Käppler, R. Gallino, S. Bisterzo, and W. Aoki, *Rev. Mod. Phys.* **83**, 157 (2011).
- 490 [11] Y. Z. Qian, *Prog. Part. Nucl. Phys.* **50**, 153 (2003).
- 491 [12] S. J. Smartt, *Annu. Rev. Astron. Astrophys.* **47**, 63 (2009).
- 492 [13] T. Faran, D. Poznanski, A. V. Filippenko, R. Chornock, R. J. Foley, M. Ganeshalingam, D. C.
493 Leonard, W. Li, M. Modjaz, F. J. D. Serduke, and J. M. Silverman, *Mon. Not. R. Astron.*
494 *Soc.* **445**, 554 (2014).
- 495 [14] T. C. Beers and N. Christlieb, *Annu. Rev. Astron. Astrophys.* **43**, 531 (2005).
- 496 [15] D. Carollo, K. Freeman, T. C. Beers, V. M. Placco, J. Tumlinson, and S. L. Martell, *Astrophys.*
497 *J.* **788**, 180 (2014).
- 498 [16] W. Tan, *Phys. Lett. B* **797**, 134921 (2019), arXiv:1902.01837.
- 499 [17] B. Fornal and B. Grinstein, *Phys. Rev. Lett.* **120**, 191801 (2018).
- 500 [18] Z. Berezhiani and L. Bento, *Phys. Rev. Lett.* **96**, 081801 (2006).
- 501 [19] Z. Berezhiani, *Eur. Phys. J. C* **64**, 421 (2009).

- 502 [20] Z. Berezhiani, R. Biondi, P. Geltenbort, I. A. Krasnoshchekova, V. E. Varlamov, A. V. Vassil-
503 jev, and O. M. Zhrebtsov, *Eur. Phys. J. C* **78**, 717 (2018).
- 504 [21] Z. Berezhiani, *Eur. Phys. J. C* **79**, 484 (2019).
- 505 [22] A. T. Yue, M. S. Dewey, D. M. Gilliam, G. L. Greene, A. B. Laptev, J. S. Nico, W. M. Snow,
506 and F. E. Wietfeldt, *Phys. Rev. Lett.* **111**, 222501 (2013).
- 507 [23] R. W. Pattie, N. B. Callahan, C. Cude-Woods, E. R. Adamek, L. J. Broussard, S. M. Clayton,
508 S. A. Currie, E. B. Dees, X. Ding, E. M. Engel, and others, *Science* **360**, 627 (2018).
- 509 [24] Z. Tang, M. Blatnik, L. J. Broussard, J. H. Choi, S. M. Clayton, C. Cude-Woods, S. Currie,
510 D. E. Fellers, E. M. Fries, P. Geltenbort, and others, *Phys. Rev. Lett.* **121**, 022505 (2018).
- 511 [25] UCNA Collaboration, X. Sun, E. Adamek, B. Allgeier, M. Blatnik, T. J. Bowles, L. J. Broussard,
512 M. A.-P. Brown, R. Carr, S. Clayton, and others, *Phys. Rev. C* **97**, 052501 (2018).
- 513 [26] M. Mannarelli, Z. Berezhiani, R. Biondi, and F. Tonnelli, in *Nordita ESS workshop* (Stockholm
514 University, Sweden, 2018).
- 515 [27] I. Goldman, R. N. Mohapatra, and S. Nussinov, (2019), arXiv:1901.07077 [hep-ph].
- 516 [28] R. Foot, *Int. J. Mod. Phys. D* **13**, 2161 (2004).
- 517 [29] Z. Berezhiani, *Int. J. Mod. Phys. A* **19**, 3775 (2004).
- 518 [30] J.-W. Cui, H.-J. He, L.-C. Lü, and F.-R. Yin, *Phys. Rev. D* **85**, 096003 (2012).
- 519 [31] A. P. Serebrov, E. B. Aleksandrov, N. A. Dovator, S. P. Dmitriev, A. K. Fomin, P. Geltenbort,
520 A. G. Kharitonov, I. A. Krasnoschekova, M. S. Lasakov, A. N. Murashkin, G. E. Shmelev,
521 V. E. Varlamov, A. V. Vassiljev, O. M. Zhrebtsov, and O. Zimmer, *Nucl. Instrum. Methods*
522 *Phys. Res. Sect. A Particle Physics with Slow Neutrons*, **611**, 137 (2009).
- 523 [32] I. Y. Kobzarev, L. B. Okun, and I. Y. Pomeranchuk, *Sov J Nucl Phys* **3**, 837 (1966).
- 524 [33] S. Blinnikov and M. Khlopov, *Sov. J. Nucl. Phys.* **36**, 472 (1982).
- 525 [34] S. I. Blinnikov and M. Y. Khlopov, *Sov. Astron.* **27**, 371 (1983).
- 526 [35] E. W. Kolb, D. Seckel, and M. S. Turner, *Nature* **314**, 415 (1985).
- 527 [36] M. Y. Khlopov, G. M. Beskin, N. G. Bochkarev, L. A. Pustilnik, and S. A. Pustilnik, *Sov.*
528 *Astron.* **35**, 21 (1991).
- 529 [37] L. B. Okun, *Phys.-Usp.* **50**, 380 (2007).
- 530 [38] W. Tan, (2019), arXiv:1903.07474 [astro-ph, physics:hep-ph].
- 531 [39] W. Tan, *Phys. Rev. D* **100**, 063537 (2019), arXiv:1904.03835.
- 532 [40] W. Tan, (2019), arXiv:1906.10262 [hep-ex, physics:hep-ph, physics:nucl-ex].

- 533 [41] W. Tan, (2019), arXiv:1908.11838 [gr-qc, physics:hep-ph, physics:hep-th].
- 534 [42] W. Tan, *Supersymmetric Mirror Models and Dimensional Evolution of Spacetime*, Preprint:
535 <https://osf.io/8qawc> (Open Science Framework, 2020).
- 536 [43] W. Tan, (2020), arXiv:2003.04687 [physics].
- 537 [44] W. Tan, *From Neutron and Quark Stars to Black Holes*, Preprint: <https://osf.io/2jywx> (Open
538 Science Framework, 2020).
- 539 [45] C. Giunti and C. W. Kim, *Fundamentals of Neutrino Physics and Astrophysics* (Oxford Uni-
540 versity Press, 2007).
- 541 [46] L. Wolfenstein, Phys. Rev. D **17**, 2369 (1978).
- 542 [47] S. P. Mikheev and A. Y. Smirnov, Sov. J. Nucl. Phys. **42**, 913 (1985).
- 543 [48] V. F. Sears, Neutron News **3**, 26 (1992).
- 544 [49] A. A. Vidotto, S. G. Gregory, M. Jardine, J. F. Donati, P. Petit, J. Morin, C. P. Folsom,
545 J. Bouvier, A. C. Cameron, G. Hussain, S. Marsden, I. A. Waite, R. Fares, S. Jeffers, and
546 J. D. do Nascimento, Mon. Not. R. Astron. Soc. **441**, 2361 (2014).
- 547 [50] C. W. Cook, W. A. Fowler, C. C. Lauritsen, and T. Lauritsen, Phys. Rev. **107**, 508 (1957).
- 548 [51] R. H. Cyburt, A. M. Amthor, R. Ferguson, Z. Meisel, K. Smith, S. Warren, A. Heger, R. D.
549 Hoffman, T. Rauscher, A. Sakharuk, H. Schatz, F. K. Thielemann, and M. Wiescher, Astro-
550 phys. J. Suppl. Ser. **189**, 240 (2010).
- 551 [52] M. Heil, R. Detwiler, R. E. Azuma, A. Couture, J. Daly, J. Görres, F. Käppeler, R. Reifarth,
552 P. Tischhauser, C. Ugalde, and M. Wiescher, Phys. Rev. C **78**, 025803 (2008).
- 553 [53] A. Best, M. Beard, J. Görres, M. Couder, R. deBoer, S. Falahat, R. T. Güray, A. Kontos,
554 K.-L. Kratz, P. J. LeBlanc, and others, Phys. Rev. C **87**, 045805 (2013).
- 555 [54] P. Mohr, Phys. Rev. C **96**, 045808 (2017).
- 556 [55] C. E. Rolfs and W. S. Rodney, *Cauldrons in the Cosmos: Nuclear Astrophysics* (University of
557 Chicago Press, 1988).
- 558 [56] B. Bucher, X. D. Tang, X. Fang, A. Heger, S. Almaraz-Calderon, A. Longi, A. D. Ayangeakaa,
559 M. Beard, A. Best, J. Browne, and others, Phys. Rev. Lett. **114**, 251102 (2015).
- 560 [57] X. Fang, W. P. Tan, M. Beard, R. J. deBoer, G. Gilardy, H. Jung, Q. Liu, S. Lyons, D. Robert-
561 son, K. Setoodehnia, and others, Phys. Rev. C **96**, 045804 (2017).
- 562 [58] B. S. Meyer, Annu. Rev. Astron. Astrophys. **32**, 153 (1994).
- 563 [59] M. Lugaro and F. Herwig, Nucl. Phys. A Nuclei in the Cosmos, **688**, 201 (2001).

- 564 [60] W. Tan, (2020), arXiv:2006.10746 [hep-ph].
- 565 [61] S. Chandrasekhar, Lond. Edinb. Dublin Philos. Mag. J. Sci. **11**, 592 (1931).
- 566 [62] National Nuclear Data Center, “NuDat 2 database,” .
- 567 [63] B. E. J. Pagel, *Nucleosynthesis and Chemical Evolution of Galaxies* (1997).
- 568 [64] O. Tarasov, R. Allatt, J. C. Angélique, R. Anne, C. Borcea, Z. Dlouhy, C. Donzaud, S. Grévy,
569 D. Guillemaud-Mueller, M. Lewitowicz, and others, Phys. Lett. B **409**, 64 (1997).
- 570 [65] R. deSouza, J. Vadas, V. Singh, B. Wiggins, T. Steinbach, Z. Lin, C. Horowitz, L. Baby,
571 S. Kuvin, V. Tripathi, I. Wiedenhover, and S. Umar, EPJ Web Conf. **163**, 00013 (2017).
- 572 [66] B. Kiziltan, A. Kottas, M. D. Yoreo, and S. E. Thorsett, Astrophys. J. **778**, 66 (2013).
- 573 [67] M. D. Delano and A. G. W. Cameron, Astrophys. Space Sci. **10**, 203 (1971).
- 574 [68] M. van der Klis, Adv. Space Res. **38**, 2675 (2006).
- 575 [69] T. Nagel and K. Werner, Astron. Astrophys. **426**, L45 (2004).
- 576 [70] R. B. Leighton, R. W. Noyes, and G. W. Simon, Astrophys. J. **135**, 474 (1962).
- 577 [71] R. K. Ulrich, Astrophys. J. **162**, 993 (1970).
- 578 [72] H.-T. Janka, Annu. Rev. Nucl. Part. Sci. **62**, 407 (2012).
- 579 [73] A. Burrows, Rev. Mod. Phys. **85**, 245 (2013).
- 580 [74] M. Markevitch, A. H. Gonzalez, D. Clowe, A. Vikhlinin, W. Forman, C. Jones, S. Murray,
581 and W. Tucker, Astrophys. J. **606**, 819 (2004).
- 582 [75] D. Clowe, A. Gonzalez, and M. Markevitch, Astrophys. J. **604**, 596 (2004).